

A 18mW, 3.3dB NF, 60GHz LNA in 32nm SOI CMOS Technology with Autonomic NF Calibration

J.-O. Plouchart¹, F. Wang², A. Balteanu¹, B. Parker¹, M. A. T. Sanduleanu¹, M. Yeck¹, V. H.-C. Chen¹, W. Woods³, B. Sadhu¹, A. Valdes-Garcia¹, X. Li², and D. Friedman¹

¹IBM T. J. Watson Research Center, Yorktown Heights, NY, USA

²Electrical & Computer Engineering Department, Carnegie Mellon University, Pittsburgh, PA, USA

³IBM Semiconductor Research and Development Center, Essex Junction, VT

Abstract—A self-healing mmWave SoC integrating an 8052 microcontroller with 12kB of memory, an ADC, a temperature sensor, and a 3-stage cascode 60GHz LNA, implemented in a 32nm SOI CMOS technology exhibits a peak gain of 21dB, an average 3.3dB NF from 53 to 62GHz and 18mW power consumption. An indirect NF sensing algorithm was implemented on the integrated uC, which enables an adaptive biasing algorithm to reduce the 60GHz NF sigma and LNA power consumption by 37 and 40%, respectively, across P,V,T.

Index Terms—Mm-wave, SoC, NF, LNA, 60GHz, autonomic calibration.

I. INTRODUCTION

The design of millimeter-wave (mmWave) transceivers in advanced CMOS technology nodes are attractive due to high f_T , f_{MAX} and its integration with complex digital circuits. However such a design remains a challenge due to device modelling uncertainties and sensitivities to process (P), supply voltage (V), and temperature (T) variations. This challenge has motivated research in the area of self-healing circuit capabilities for mmWave circuits [1]-[2]. Note, however, that mmWave transceiver (TRx) measurements are difficult even using external measurement equipment, and further that integrating on-chip direct mmWave measurement infrastructure is in most cases not feasible. A potential solution to this problem presented in [3] is to perform indirect performance sensing by using a set of easily measurable metrics (e.g., DC bias current) to predict performance metrics of interest that are difficult to measure directly using on-chip sensors. An indirect VCO phase noise performance sensing method was demonstrated in [4], here to adaptively tune a VCO to improve its performance and/or yield. A 1.5GHz and 2.4GHz LNAs with linearity and gain [5] and S11/S21 healing capabilities [6] were also reported. For mmWave LNA noise figure (NF), a self-healing approach was presented and evaluated through simulations in [7]. In this work, we present the hardware implementation and measurements results for a self-healing 60GHz LNA.

II. MMWAVE SOC LNA DESIGN

Fig. 1 shows the SoC LNA block diagram and the detailed cascode amplifier stage schematic. The overall

design was implemented in a 32nm SOI process. The implementation of on-chip healing algorithms requires complex SoC design, especially for a mmwave TRx. In this architecture, the serial interface and microcontroller data flows are multiplexed such that the algorithm can be run either outside of the chip on a host or inside the chip on the microcontroller.

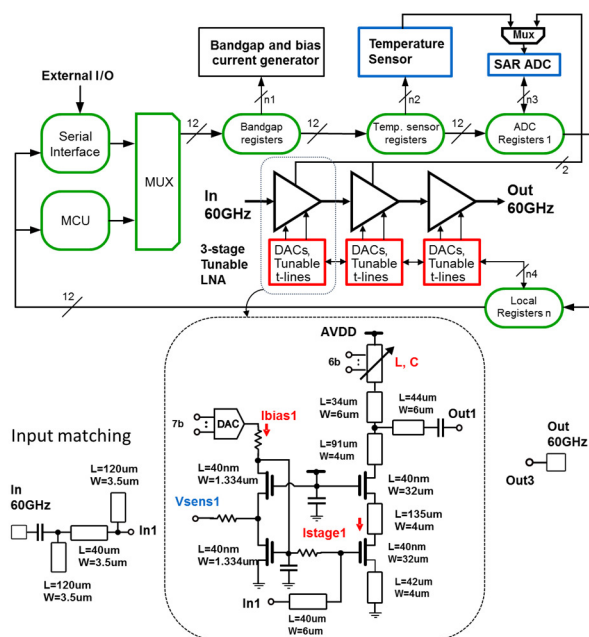


Fig. 1. Circuit block and cascode amplifier stage schematic.

A microcontroller was chosen for the healing implementation because it offers the flexibility to enhance the algorithm once the chip is tested or in the field, providing additional configurability as compared to a dedicated/fixed algorithm implementation in hardware. The healing architecture is scalable to a large number of circuits, or a full TRx, as well as an array of TRx. Since the uC, the T sensor, and the ADCs would be shared by all the circuits, the ratio between the circuit area dedicated to self-healing and the TRx area decreases as the TRx gets more complex. The uC with its 12kB of memory occupies only 0.25x1mm²,

which is a significant fraction of the LNA area, but a small fraction of the area required for a full mmWave TRx. Note that one limitation of this approach is that since the uC clock frequency is in the MHz range, the self-healing loop latency will inevitably be in the usec range, which is sufficient for most of the self-healing applications but not for applications demanding ultra-fast feedback.

The LNA itself consists of an input matching networks and three identical cascode amplifier stages. Each individual cascode amplifier stage integrates two actuators. The first of these is the DAC actuator which allows bias current adjustment. The second actuator is the digital control that enables the inductance and capacitance of the transmission line used in the cascode amplifier load to be varied [8]. The digitally tuneable line is used to tune the frequency response of the amplifier. The sensor is the ADC used to convert the voltage V_{sens1} , which tracks the DC voltage between the drain of the input stage and the source of the output stage. The FETs, along with all the wire parasitics, were extracted from the layout to enable accurate simulation. The circuit was simulated using high frequency models for the transmission lines, capacitors, and resistors used in the design.

III. MEASUREMENT RESULTS

Fig. 2 shows the LNA measured S-parameters as function of frequency and two TLine states for a supply voltage AVDD of 1.1V for the analog circuits.

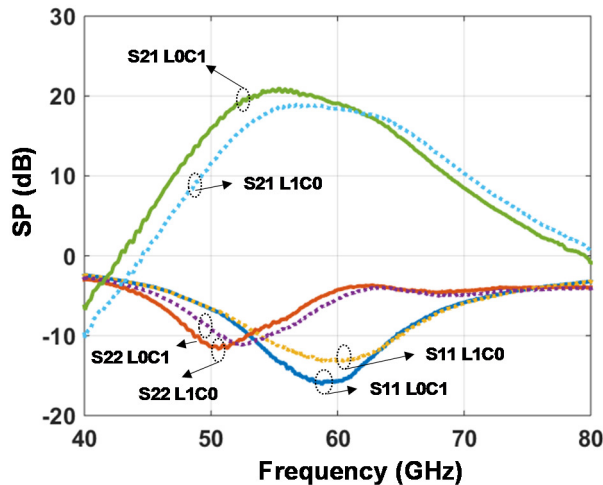


Fig. 2. Measured S-parameters for the low and high frequency TLine states at $T=25c$ and $AVDD=1.1V$.

The measured peak gain is 21dB at 55.4GHz for the L0C1 tuneable TLine state. In that state, the tuneable TLine capacitors are all turned on and the inductors are all turned off. In the opposite L1C0 state, the tuneable TLine capacitors are all turned off and the inductors are all turned on. The 3dB cut-off frequency are 51.3, 61.8GHz and 52.6,

65.1GHz for the L0C1 and L1C0 tuneable TL states, respectively. This is equivalent to a L0C1 to L1C0 frequency variation of 1.3 and 3.3GHz at the low and high frequencies, respectively. The measured input match is better than 10dB from 53 to 64.6GHz.

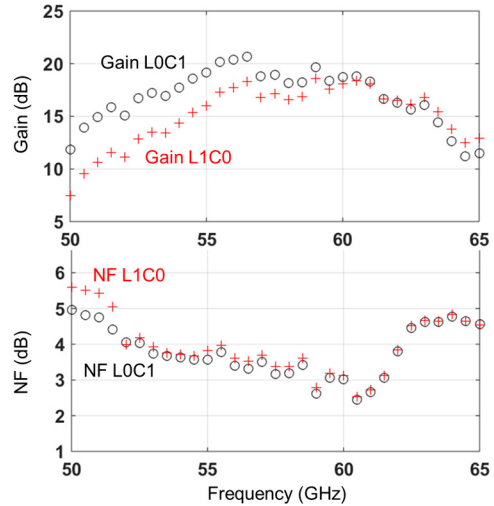


Fig. 3. Noise diode and spectrum analyzer measurements for gain and NF at $T=25c$, $AVDD=1V$, for low and high-frequency TLine states.

The NF was measured by turning on and off a mmWave noise diode and measuring the noise difference with a spectrum analyzer. A low-noise mmWave amplifier was used in front of the spectrum analyser to increase the measurement sensitivity. The input and output cable losses were measured and de-embedded from the measurements. The measured average NF from 53 to 62GHz for the L1C0 TLine state is 3.3dB at a power consumption of only 18mW from a 1V supply. The average NF degrades by 0.1dB to 3.4dB when the TLine is set to the opposite L0C1 state. The gain measured by the spectrum analyzer is consistent with the measured S21 for L0C1 and L1C0.

The NF measured at 60GHz across the total LNA bias current I_{lna} from the AVDD voltage supply, at three different supply voltages of 0.9, 1 and 1.1V and three different temperatures 25, 45 and 65c is shown in the marker points plotted in Fig. 4. The 60GHz NF predicted by the algorithm run on the uC and based on the DAC LNA bias current setting, temperature and voltage V_{sens1} and sensor measurements are shown in solid lines (Fig. 4). The equation-based NF estimation through indirect sensing was extracted by first simulating the LNA NF across P,V,T using performing Monte Carlo simulations. The NF as a function of the LNA stage current I , the temperature T , and the V_{sens1} voltage V was then fitted using a multivariate polynomial, where the orthogonal matching pursuit algorithm was used to adaptively select a small number of important polynomial terms.

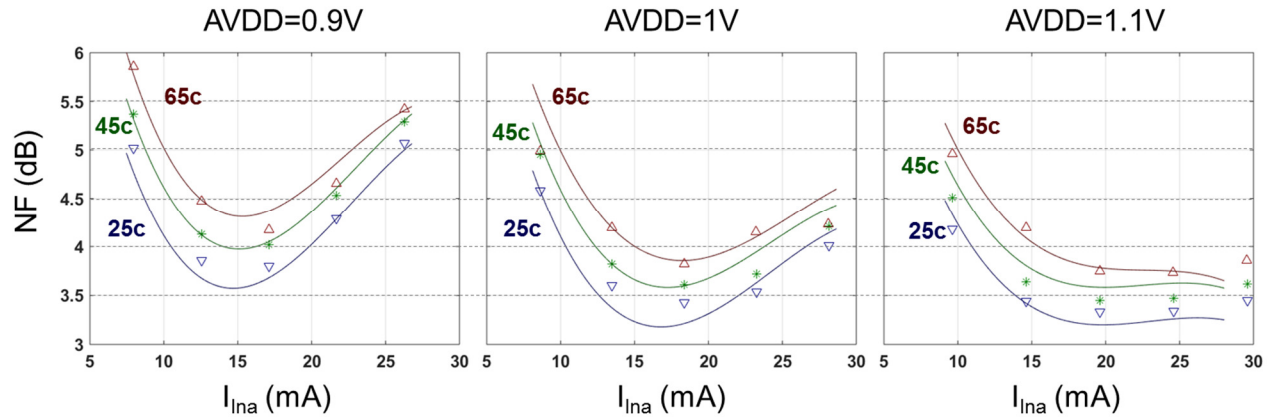


Fig. 4. 60GHz NF predicted from sensors measurements by uC (solid curves) versus measured NF (markers) across T, V, I for 1 chip.

As some discrepancy between the model derived from Monte Carlo simulations and the measured data at high current was observed, we used Bayesian model fusion as described in [9] to improve the correlation between the predicted NF and the measured NF at high current density. This methodology allows us to compensate for model inaccuracies that are likely to be present, especially at mmWave frequency. The NF equation as a function of the indirect measurements was implemented on the LNA uC with compiled C code with floating point arithmetic.

The 60GHz NF was also measured across supply voltage, bias current, and temperature for 9 different chips to evaluate the algorithm across not only supply voltage, bias current and temperature but also process variations (Fig. 5).

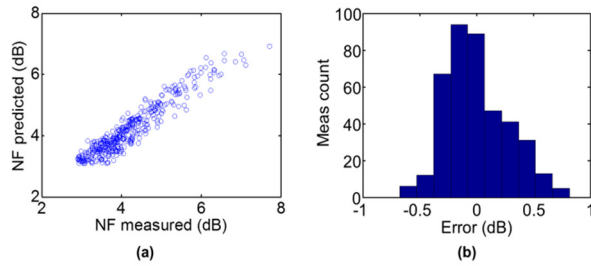


Fig. 5. (a) NF predicted from sensor measurements versus NF measured at 60GHz across P,V,T,I and (b) error histogram.

For a total of 9 chips, three voltage supplies (0.9, 1 and 1.1V), three temperatures (25, 45 and 65c), and five bias currents, NF measurements at 60GHz were made. This set of 405 results was compared with the predicted 60GHz NF measurements based on the on-chip temperature and Vsens1 voltage measurements. The error on-chip indirect sensor 60GHz NF measurement as compared to the external 60GHz NF measurement has a standard deviation of 0.28dB across P,V,T,I. This level of accuracy for on-chip mmWave NF measurement can enable mmWave receiver with unique healing and/or adaptive capabilities.

For example, assume a 60GHz NF of 5dB is specified and needs to be achieved across P,V,T. For a fixed current biasing of 18mA, all the chips exhibit a $NF \leq 5dB$ across V,T for a mean power of 18mW (Fig. 6 (a) and (b)).

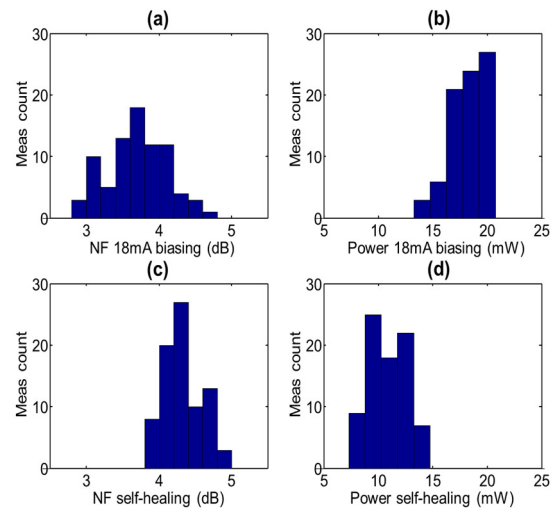


Fig. 6. Measured 60GHz NF distribution (a) and power distribution (b) across P,V,T at a fixed bias current, and measured NF (c) and power (d) distribution after healing algorithm selects the minimum power such that $NF \leq 5dB$.

The same 100% yield can be achieved with adaptive biasing using the self-healing algorithm, with the significant benefit that the mean power consumption is reduced by 40% to 10.8mW (Fig. 6 (b) and (d)). The 60GHz NF sigma is also reduced by 37% from 0.41 to 0.26dB by using adaptive LNA biasing. This example demonstrates the potential for self-healing chip to adapt to complex environmental changes and optimize its power consumption.

The measured output 1dB compression point is -4dBm. The measurements are summarized in table I.

Fig. 7 shows the mmWave LNA SoC including the uC, SRAM, serial interface, bandgap, PTAT, T sensor and SAR ADC. The chip area is 1.94mm by 1.12mm.

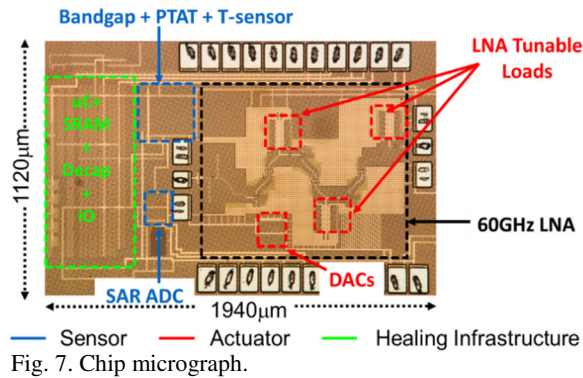


TABLE I: MEASUREMENT RESULT SUMMARY

	Measurement
Freq (GHz)	60
AVDD (V)	0.9 - 1.1
T (C)	25 - 65
Mean NF (dB) at Ilna=18mA	3.7
sigma NF (dB) at Ilna=18mA	0.41
Min/Max NF (dB) for 9 chips at Ilna=18mA	2.94 / 4.76
Mean power (mW) at Ilna=18mA	18
On chip indirect sensor NF RMS error (dB)	0.28
Mean NF (dB) for 5dB NF spec	4.32
sigma NF (dB) for 5dB NF spec	0.26
Min/Max NF (dB) for 5dB NF spec	3.83/4.87
Mean power (mW) for 5dB NF spec	10.78
Peak Gain (dB)	21
3dB BW with tunable TL low/high (GHz)	10.6 / 12.5
3dB frequency shift with tunable TL low/high (GHz)	1.3 / 3.3
Average NF from 53 - 62 GHz (dB)	3.3
OP1dB (dBm)	-4
Chip area (mm ²)	2.2
Technology	32nm SOI

To the best of the author's knowledge, the lowest reported NF for 60GHz Si-based LNAs are between 4 and 5.5dB [10]-[13], which are higher than the measured average 60GHz NF of 3.3dB for this 32nm SOI LNA.

IV. CONCLUSION

A self-healing 60GHz LNA was demonstrated in a 32nm SOI CMOS technology. The measured peak LNA gain is 21dB at 55.4GHz, and an average 3.3dB NF from 53 to 62GHz is measured for a power consumption of only 18mW on a 1V supply. The healing algorithm was implemented on the integrated uC. Good agreement between the self-healing NF predicted from DC measurements and the external 60GHz NF measurements was achieved over a broad LNA bias current voltage supply and temperature range. This demonstrates that difficult mmwave measurements such as NF can be performed indirectly and integrated efficiently on-chip. These results

are an important step towards self-adaptive TRx circuits and systems that can minimize energy needed to transmit and receive under varying environmental conditions.

ACKNOWLEDGMENT

The authors thank Roger Moussalli for support with uC evaluation. This work is sponsored by the DARPA HEALICS program under Air Force Research Laboratory (AFRL) contract FA8650-09-C-7924. The views expressed are those of the author and do not reflect the official policy or position of the Department of Defense or the U.S. Government.

REFERENCES

- [1] C. Maxey, G. Creech, S. Raman, and J. Rockway, "Mixed-signal SoCs with in situ self-healing circuitry," *IEEE Design & Test of Computers*, vol. 29, no. 6, pp. 27-39, Dec. 2012.
- [2] C. Chien et al., "Dual-control self-healing architecture for high-performance radio SoCs," *IEEE Design & Test of Computers*, vol. 29, no. 6, pp. 40-51, Dec. 2012.
- [3] S. Sun et al., "Indirect Performance Sensing for On-Chip Self-Healing of Analog and RF Circuits," *IEEE Transactions on Circuits and Systems*, vol. 61, no. 8, pp. 2243-2252, Aug. 2014.
- [4] B. Sadhu et al., "A linearized, low-phase-noise VCO-based 25-GHz PLL with autonomic biasing," *IEEE Journal of Solid-State Circuits*, vol. 48, no. 5, pp. 1138-1150, May 2013.
- [5] S. Sen et al., "A power-scalable channel-adaptive wireless receiver based on built-in orthogonally tunable LNA," *IEEE Transactions on Circuits and Systems*, vol. 59, no. 5, pp. 946-957, May 2012.
- [6] K. Jayaraman et al., "A self-healing 2.4GHz LNA with on-chip S11/S21 measurement/calibration for in-situ PVT compensation," *IEEE RFIC Symposium*, Jun. 2010, pp. 311-314.
- [7] J.-O. Plouchart et al., "Adaptive Circuit Design Methodology and Test Applied to Millimeter-wave Circuits," *IEEE Design & Test*, issue 99, 2014.
- [8] W. H. Woods et al., "CMOS Millimeter Wave Phase Shifter Based on Tunable Transmission Lines," *IEEE Custom Integrated Circuits Conference*, pp. 1-4, Sep. 2013.
- [9] F. Wang et al., "Bayesian model fusion: large-scale performance modeling of analog and mixed-signal circuits by reusing early-stage data," in *Proceedings of Design Automation Conference*, pp. 1-6, Jun. 2013.
- [10] H-H Hsieh et al., "60GHz High-Gain Low-Noise Amplifiers with a Common-Gate Inductive Feedback in 65nm CMOS," *IEEE RFIC Symposium*, Jun. 2011, pp. 1-4.
- [11] T. Yao et al., "Algorithmic Design of CMOS LNAs and PAs for 60-GHz Radio," *IEEE Journal of Solid-State Circuits*, vol. 42, no. 5, pp. 1044-1057, May 2007.
- [12] B. A. Floyd et al., "SiGe bipolar transceiver circuits operating at 60 GHz," *IEEE Journal of Solid-State Circuits*, vol. 40, no. 1, pp. 156-157, Jan. 2005.
- [13] M. Uzunkol and G. M. Rebeiz, "A 65 GHz LNA/Phase Shifter With 4.3 dB NF Using 45 nm CMOS SOI," *IEEE Microwave and Wireless Components Letters*, vol. 22, no. 10, pp. 530-532, Oct. 2012.